Influence of adsorbates, crystal structure, and target temperature on the sputtering yield and kinetic-energy distribution of excited Ni atoms

A. Cortona, W. Husinsky, and G. Betz
Institut für Allgemeine Physik, Vienna University of Technology, Wiedner Hauptstrasse 8-10, A-1040 Wien, Austria
(Received 11 January 1999)

We present results for the emission of secondary Ni atoms in the electronic ground state and some excited metastable states under ion bombardment. In particular, we address some of the most urgent questions resulting from previous measurements of the Ni system: the influence of adsorbates, in particular oxygen, on the excitation, the influence of the crystal structure and orientation, and possible temperature effects. A direct comparison between sputtering under identical experimental conditions from polycrystalline and single crystal targets has been performed. Inelastic processes have been found to play an important role in determining the population of the different electronic levels of sputtered atoms. The density of states of the solid and the overlap of the electronic wave functions of the atom and the solid (bulk or surface) determine the efficiency of the population of individual atomic levels and the energy distribution of the atoms in these electronic states. Analyzing the experimental data, the contribution of inelastic processes to elastic cascade sputtering for clean, oxidized, and carbonized surfaces, at room temperature and up to 800 °C as well as for various azimuthal angles could be determined and has finally led to a coherent description of the sputtering-excitation process for low-lying excited Ni atoms: the emission of an ionic core and subsequent electron capture into excited states. [S0163-1829(99)07823-6]

I. INTRODUCTION

Inelastic mechanisms involved in sputtering of metals as a consequence of ion bombardment in the keV range are still not completely understood. While it is believed that elastic processes, which often dominate the sputtering process, can be pretty well described by existing models[1–3] and computer simulations,[4] inelastic processes can be of quite considerable importance in specific situations.

In particular, the emission of secondary excited particles is a typical situation where inelastic and electronic processes are involved. Experimental results obtained in the past few years[5–11] have considerably broadened the understanding of the processes leading to emission of secondary excited particles, but the present knowledge still can be regarded as rather rudimentary in many aspects.

Sputtering of excited metastable Ni atoms has been the focus of several investigations in the past few years since, due to its specific electronic structure, this system allows one to test many of the models proposed over the years. In this paper we will present results for the emission of Ni atoms in the electronic ground state and some excited metastable states under ion bombardment. In particular, we will address some of the most urgent questions resulting from previous measurements of the Ni system: the influence of adsorbates, in particular oxygen, on the excitation, the influence of the crystal structure and orientation, and possible temperature effects. Concerning the role played by the target crystalline structure, most experiments reported in the literature have been performed on either polycrystalline or single crystal targets, but no direct comparison between sputtering under identical experimental conditions from polycrystalline and single crystal target has been performed so far; this will be discussed in the present paper.

The existence of excited atoms and molecules as a consequence of ion bombardment of solids is a well known phenomenon and has been studied for a long time; one of the most remarkable results obtained from the measurements of sputtered excited metastable Ni atoms, from both polycrystalline and single crystal targets, is the pronounced population inversion of some electronic states, with very low excitation energies, with respect to the electronic ground state. Other experiments[12–14] have established the general understanding that oxygen or other electronegative adsorbates on the surface of the bombarded material have a crucial and significant influence on the yield of excited particles after ion bombardment.[15,12,14,16]

Early measurements investigated the light emission vs distance from the target and lead to controversial results.[17–20] The picture of the excitation process was modified considerably with the availability of laser induced fluorescence[21] (LIF) experiments.[22–24] They modified our picture insofar that it was believed that atoms sputtered in excited metastable states with a few eV excitation energy are characterized by kinetic energies above those typically found for ground state atoms. Atoms in states belonging to the ground state multiplet have been observed to have energies very close or identical to those predicted by the Sigmund-Thompson distribution,[3,25] while atoms in levels with a few eV potential energy typically have higher emission velocities. This was explained by means of a selective, nonradiative deexcitation of excited atoms near the surface.

In the past few years, however, the sensitive method of resonant ionization spectroscopy[5,26,27] (RIS) has shown that our previous understanding was rather crude and the description of the physics of the excitation process has to be modified in many ways.[5–11] In addition, the influence of oxygen turned out to be rather puzzling and different from previous knowledge.

TABLE I. Used Ni transitions.

Initial state (cm^{-1})	Intermediate state (cm^{-1})	Photon energy (cm^{-1})	g_i	g_k	A_{ki} (10^8 Hz)	Final energy above the g.s. (cm^{-1})
$a\ ^3F_4$ (0.0)	$z\ ^3G_4^0$ (30979.7)	30979.7	9	9	0.0023	61960
$a\ ^3D_3$ (204.8)	$z\ ^3G_4^0$ (30979.7)	30775.2	7	9	0.0047	61766
$a\ ^3D_2$ (880)	$^3F_3^{0*}$ (33112)	32232	5	7	0.63	65344

There is now strong evidence that the electronic configuration of the emitted particle and the electronic band structure of the solid are decisive elements in determining the emission probability in a specific state and also its velocity distribution. In other words, inelastic processes, such as velocity- and state-dependent energy transfer, come into play.[8–11]

This statement can also be made in the reverse way: The velocity of the emitted particle will influence the electron capture probability in a specific level, thus the excitation probability. The velocity distribution, together with measurements of the state-specific yield, can be used as a very sensitive tool to probe excitation models and obtain information about electronic processes involved in the excitation process.

II. SPECTROSCOPY OF THE Ni I SYSTEM

Nickel has been chosen as an experimental sample for its interesting energy level arrangement at low energies: Levels belonging to the first excited multiplet D_J and to the ground state F_J multiplet are energetically nearly identical, but their electronic configuration is different. This makes Ni one of the few elements where analogies and differences in the excitation probability for levels with different electronic configurations but similar excitation energy can easily be experimentally investigated. The continuum level for Ni lies 7.635 eV above the ground state, thus two photons in the visible range are needed to ionize ground state atoms: We realized two-step resonant photoionization of sputtered atoms using a tunable Dye Laser FL3002 from Lambda Physik. The laser was operated with rhodamine B and DCM dye, whose operating regime ranges from 588 to 644 nm and from 632 to 690 nm, respectively, making it necessary to double the fundamental wavelength with a KDP frequency doubler.

At this point, we should distinguish between resonant (RIS) and nonresonant (NRIS) postionization, in which only the excitation step of the two-photon transition is resonant or nonresonant. While operating in the RIS mode a narrow-band dye laser pulse with an average power of approximately 10^8 W/cm^2 is used. The laser resonantly excites atoms from the initial state to an intermediate state, a discrete bound state, and then photons with the same color ionize the atoms from the intermediate to a state above the first ionization limit.

When operating in the NRIS mode, on the other hand, we used an excimer laser operated with XeCl. It produces an intense but relatively broadband pulse at 308 nm; the resonance condition is generally not satisfied for most elements. The second photon transition, which transfers the electron from the excited bound state above the ionization limit, is generally nonresonant. However, it is well known that the continuum above the first ionization limit is not a real continuum, but rather a quasicontinuum; the first ionization limit is in fact valid only for an atom in the ground state. This gives rise to a set of discrete states embedded in the continuum above the first ionization energy; these states are properly called Rydberg states or autoionizing states.

The existence of autoionizing states for Ni has been experimentally proved by measurements[28] realized with a two-step, two-color ionization experiment, where the photoion yield was recorded vs the ionizing laser wavelength.

Very strong lines with the typical Fano profile have been observed; some of them were found out to be coincident with Rydberg states lying above the first ionization limit, while others were interpreted as a result of a two-electron excitation and subsequent ionization. In other words, if the final state is an autoionizing level, a quasiresonant ionization takes place and the corresponding transition efficiency is two to three orders of magnitude higher than for a transition ending up in an unstructured continuum. The situation is the same as the one described for the excitation step.

For the measurements presented in this paper, only one tunable laser source was available. However, in the case of Ni one can select the wavelength of the first resonant excitation step in such a manner that it also coincides in some cases with a transition to an autoionizing state for the second photon. The spectroscopic properties of photoionization transitions used in our experiment are listed in Table I; the energetic states involved are indicated together with the excitation energy and multiplicity for each level and the Einstein coefficients A_{ki} for spontaneous emission between bound states. Note that for nickel the first ionization potential lies at 61 600 cm^{-1}; the autoionizing states lie, as expected, just above the first ionization limit.

III. EXPERIMENT

Polycrystal and single crystal Ni targets were bombarded under a polar angle of incidence of 45° M/J with Ar^+ ions of 8.0 keV energy and 1.5 μA current from a cold-cathode ion source; the primary ion flux density was around 10^{16} Ar^+ions/s cm^2. The base pressure in the UHV chamber was approximately 10^{-9} mbar.

Since the yield of atoms sputtered in excited states might strongly depend on the presence of impurities, in particular oxygen, on the surface, it was necessary to clean the sample. This was achieved *in situ* by sputtering with a continuous ion beam, which was rastered across a surface area of about 2×2 mm^2 for a few minutes before the measurement. Secondary ion mass spectroscopy (SIMS) could be used to check the surface composition with respect to impurities, in particular oxides. Within the sensitivity of SIMS no measurable surface contaminations have been detected. Therefore, for measurements with a continuous dc primary ion beam, the influence of oxygen or other impurities can be assumed to be minimal. For measurements of the velocity distribu-

TABLE II. Population partition on clean Ni.

Initial state (cm^{-1})	Population relative to the ground state
$a\ ^3F_4\,(0.0)$	1
$a\ ^3D_2\,(880)$	0.96
$a\ ^3D_3\,(204.8)$	1.19

tions, where the ion beam has to be pulsed, regular dc sputter cleaning also ensured clean surfaces.

Ionization of secondary neutral atoms was achieved with the focused laser beam whose center axis runs parallel to the sample at a distance d of approximately $2-4$ mm. The laser focus was approximately 0.2 mm in diameter.

After postionization the particles were accelerated and mass analyzed in a time-of-flight (TOF) spectrometer. Measurements were performed with two different geometries. One geometry with an ion mirror was used to reflect the photoions onto the channel-plate detector. This operating mode yields high mass resolution and suppresses secondary ions created at the target surface. This operating mode was generally used for yield measurements, while for velocity measurements a straight line TOF geometry was used in order to avoid velocity dependent transmission effects of the TOF spectrometer.

The (TOF) of secondary neutral atoms from the sample surface to the ionization volume ($d \approx 2-4$ mm) is determined by setting a certain delay t between the primary ion pulse and the laser pulse. Thus only particles with a flight time t from the target to the laser are ionized. Measuring the exact distance d allows determination of the particle velocity v.

In order to obtain a high time resolution, it was necessary to use very short ion pulses with a half width of less than 100 ns. This is much shorter than the characteristic drift times, except for very high particle velocities.

Only particles emitted within a narrow angle around the surface normal were detected with the TOF spectrometer. Therefore, all secondary neutral atoms have nearly the same drift length d from the surface to the ionization volume. A more detailed description of the experimental details has been previously presented.[5,29]

IV. POPULATION OF EXCITED METASTABLE STATES

A. Room temperature

The measurement of the population of particles in excited states emitted in a sputter event has been a challenging task especially as far as absolute yields or even the relative population of levels are concerned. One of the most astonishing findings recently obtained from measurements for several low-lying levels of Ni and Co (Refs. 10, 11, and 30) is that the ground state is not necessarily the state with the highest population. This population inversion implies electronic excitation processes, which is the main subject of the present paper. Since only very few experiments have addressed this issue, we have started our investigations, which will be presented here, with a verification of these findings.

Experimental population densities for Ni atoms sputtered in metastable states are shown in Table II. In good agreement with similar results mentioned above,[10,11,30] we also found a population inversion between states belonging to the open-shell ^3D_J multiplet and the closed-shell ^3F_J ground state multiplet.

To evaluate the reliability of these results, it is important to state that different postionization schemes have been used: (a) two-photon one-color ionization to the continuum, (b) two-photon two-color ionization to autoionizing states, and (c) two-photon one-color ionization to autoionizing states. In addition, various intermediate levels have been used.

In our measurements we have used schemes (a) and (c). In (a), where the ionization cross sections differ by orders of magnitude for different lines, the signals have been calibrated using a thermal Ni beam. It is particularly noteworthy that all methods yield basically the same results as far as the population inversion is concerned.

A reasonable explanation for the population enhancement in the ^3D_J multiplet might be the fact that the Ni bulk configuration is more d-like than s- or p-like. As a consequence, the overlap and the cross section for electron exchange between d states is considerably larger than for the s-like ground state of Ni. The experimental evidence of the population inversion proves that evidently the electron exchange cross section is much more of a determining factor than the energy of the level itself.

It is also interesting to compare the influence of the crystallographic structure on these results. We have performed the measurements for polycrystalline and a Ni[100] single crystal and found in both cases the same result as far as the population inversion is concerned. In a later section we will present data on the angle of incidence dependence.

B. Temperature dependence

1. State-selective resonant detection

Since the population of a level with a particular energy in the absence of electronic interactions is determined by the temperature, it seems to be interesting to study the influence of the target temperature during ion sputtering on the population of the metastable levels. If the interaction of the particle (*ion in this case*) leaving the surface with the valence band electrons is the determining factor for the population of the level, the direct influence of the target temperature is expected to be low.

In this context we will exclusively explain our results by this model since most of the other models fail to explain at least some of the experimental findings. For the models suggested by Kelly,[31] Yu,[32] Craig *et al.*,[33] and others a temperature influence might be considerably larger. According to the random energy transfer model, the excitation and kinetic energy are transferred to the emitted atoms (not ionic cores) in the last collision: A temperature effect, such as a modification in the population partition or even to some extent in the kinetic energy transmitted in the last collision, could be imaginable in this scenario.

To examine in more detail the role played by the bulk and surface electronic configuration (i.e., the density of states of s-, p-, and d-like electrons) we performed measurements of the population densities for different target temperatures on a Ni[100] single crystal. The amount of neutral atoms sputtered in the Ni I ground state and $a\ ^3D_3$ excited state as a

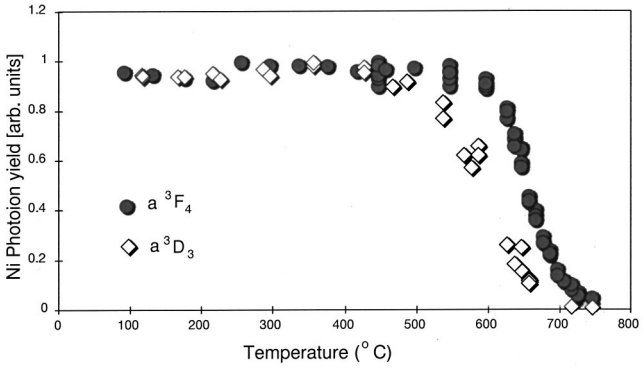

FIG. 1. Photoion signal as a function of the target temperature for sputtered Ni atoms in the ground state and $a\ ^3D_3$ metastable state. The target was sputter cleaned at every temperature before taking the data. The signals are normalized to one at room temperature.

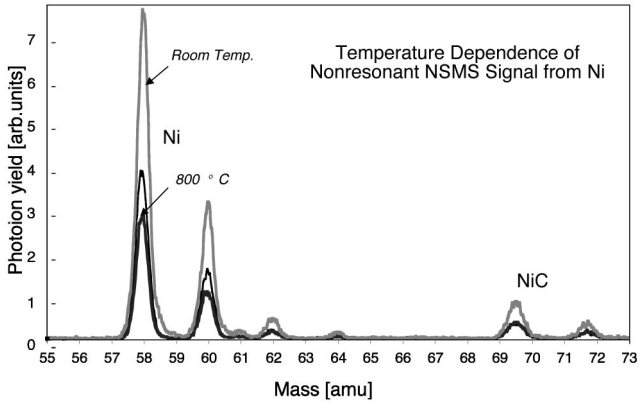

FIG. 2. Neutral secondary mass spectrum (NSMS) of neutral particles emitted from the Ni target at different temperatures. All mass spectra were measured in a NRIS laser TOF spectrometer in the reflectron mode.

function of the target temperature is shown in Fig. 1. The yield for both levels (*in the figure the signals are normalized and therefore the population inversion is not directly visible*) remains practically constant up to about 500 °C. From this we can conclude that the temperature induced population of the levels is negligible as compared to the electronic effects during the sputtering process.

The strong drop of the yield for atoms in either of the two electronic configurations measured here between 500 °C and 600 °C is remarkable and has no straightforward explanation. Above 700 °C the signal has dropped at least by a factor of 100. One might speculate about the reasons for this drop, but the most plausible hypothesis to explain the drastic decrease of the Ni signal is the diffusion of carbon from the bulk to the target surface, modifying its physical properties, such as the structure or surface electron density. In particular, C will lead to a carbonization of the surface. The surface binding energy of a Ni atom to a carbonized surface is generally higher than to a metallic surface. This results in a lower sputtering yield of Ni atoms. Together with the reduced surface concentration of Ni, a reduction of the Ni signal by a factor up to 5 could be explained in this manner. However, this is not sufficient to understand the experimentally observed decrease of Ni atoms in the low-lying electronic states.

Since the signal in Fig. 1 corresponds to atoms in low-lying metastable states, one might speculate that at higher temperatures higher-lying states are increasingly populated. This possibility has to be taken into account and will be discussed later. Another possibility would be the predominant emission of molecules,[23,34] i.e., NiC^+.

2. Nonresonant detection of total yield

In order to address these two questions in more detail one obvious approach is to measure, with NRIS, the total neutral sputtering yield as a function of the target temperature. The measurement of the velocities of the sputtered Ni atoms, together with the recording of the mass spectrum of the sputtered particles, is a sensitive tool to probe modifications in the surface structure and electron density. This can in fact help to identify the physical processes that lead to the decrease of the yield.

The total sputtering yield after ion bombardment comprises all emitted species, such as neutral atoms, in either the ground or excited states, ions, clusters, and molecules; the mass spectrum can be measured by NRIS. (TOF) spectroscopy discriminates between different masses. As the ionization takes place nonresonantly, the signal for each element isotope includes atoms in all electronic states. Furthermore, the different ionization cross sections for the various electronic states will determine how far each level will contribute to the total signal.

In other words, interpreting the signals obtained in this operating mode is not an easy task and might obscure the conclusions. An even stronger ambiguity can arise from photo-fragmentation of molecules containing Ni atoms. In fact, it can happen that one of the fragmented species is a positively charged Ni atom, which is detected in the same atomic mass channel as a sputtered neutral Ni atom (for details see Ref. 35).

So far, measurements of state selective RIS-secondary neutral mass spectroscopy from the ground state and one low-lying Ni level were presented: We have seen that the population of low-lying metastable states vanishes between 600 °C and 700 °C. Measuring the total yield in the nonresonant mode described above, we observe a totally different picture. In Fig. 2 mass spectra of neutral atoms at different temperatures are shown. The Ni peaks decrease in height to about 30%. The presence of a NiC peak in the mass spectrum is an indication that carbon is present at the surface. The quantification of the NiC is, however, difficult since fragmentation during the ionization can totally obscure the quantitative information. Furthermore, it is difficult to relate the NiC peak directly to the C concentration on the surface.

Sputtered ions can to some extent be regarded as a limit case of sputtered excited atoms. It is therefore interesting to measure the temperature dependence of the ionic species. We have measured the secondary ion mass spectrum at different temperatures (see Fig. 3).

At high temperatures we can clearly observe that the Ni ion emission is suppressed by more than 50% and that other low masses such as carbon, sodium, potassium, and aluminum show up. This partially confirms the expectation that carbon migrates to the surface building carbides, thus reducing the pure Ni surface; this could then explain the decrease

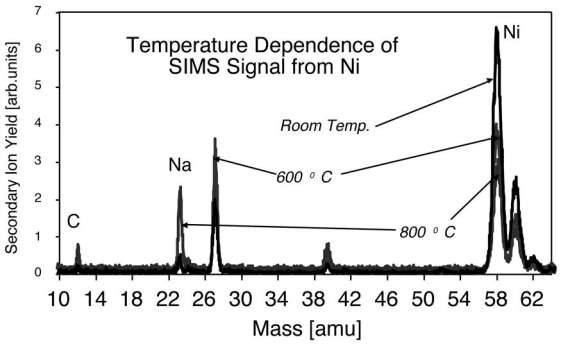

FIG. 3. Mass spectrum of ionic particles emitted from the Ni target at different temperatures. All mass spectra were measured in a NRIS laser TOF spectrometer (in the SIMS mode). C as well as Na, K, and Al impurities increase with the temperature; Ni atom emission decreases with increasing temperature.

in the emission of a factor $2-3$ that has been found for the neutral Ni atoms by NRIS (see Fig. 2). However, this still cannot explain the strong population density decrease observed for low-lying states.

In conclusion, the experimental data could be explained either with an altered population partition at increasing temperature due to thermal processes that are independent from the electronic tunneling processes. Another possible responsible factor could be the presence of other elements, such as C, on the surface. These elements could modify the electron density at the surface in such a way that the tunneling probability into high-lying states is much more favorable than into low-lying states.

Finally, the Ni and Ni_2 signal observed in nonresonant measurements can also originate from photodissociation of Ni clusters or molecules containing Ni that end up in the same mass channel as neutral Ni atoms emitted as individual atoms.

V. INFLUENCE OF SURFACE OXIDATION ON THE POPULATION PARTITION

We measured the Ni photoion yield dependence on the oxygen coverage on the surface. The target was exposed to an increasing O_2 partial pressure. The partial pressure in the chamber was varied from the residual partial pressure in the chamber under normal conditions ($\leqslant 10^{-10}$ torr) to a maximal value of 10^{-4} torr. Since the ion beam pulse was approximately 100 ns long, the erosion rate was minimal and the oxygen pressure range mentioned above covers the equivalent from a clean to a fully oxidized surface.

Previous experiments, performed with Doppler LIF spectroscopy, showed a distinctive increase of light emission for higher excited states and relatively little change for levels of the ground state multiplet. Our yield vs pressure measurements of particles in the ground and the metastable $a\ ^3D_3$ show that the yield decreases slightly between 10^{-7} and 10^{-4} torr (Table III). The decrease is stronger for atoms belonging to the $a\ ^3F_4$ ground state. Similar data reported by other RIS experiments[30] show the same trend.

The presence of oxygen atoms on the surface induces stoichiometric modifications but also alterations of the electronic configuration.To interpret the experimental results, we

TABLE III. Populaiton partition on oxidized Ni.

Initial state (cm^{-1})	Population relative to the clean Ni surface
$a\ ^3F_4\,(0.0)$	0.27
$a\ ^3D_3\,(204.8)$	0.58

used calculations of the average bulk density of states (DOS) for NiO and Ni, which have been obtained with the WIEN97 program, based on the linear plane wave approximation.[36]

The electronic density of states is calculated in a sphere around each atom of a crystal separately for *s*-like, *p*-like, and *d*-like electrons; the sum of all these functions is equal to the total density of states in the sphere around the Ni core. Furthermore, the density of states in the interstitial space is determined; the weighted sum of the latter two quantities is the total average density of states. This argument is a rather delicate one; we should, in fact, consider that on an oxidized surface the electrons might be concentrated close to the electronegative element and consequently the region in the surrounding of the escaping metallic core will be depleted.

In the case of a Ni solid, the local and the average density of states are practically the same, while this is not the case for a NiO solid. In both cases the *d*-like electrons are by far the predominant electrons in the solid (out of every ten electrons, 9.6 are in the *d*-like configuration). For this reason we compared for Ni and NiO the local density of states (instead of the average DOS) for *d*-like electrons in the same sphere around the atomic core (Fig. 4).

We focused our attention on the region approximately 2.7 eV below the Fermi energy of Ni. This corresponds to the ground state for a Ni free atom. It is evident that the local *d*-like DOS is higher for a NiO sample than the corresponding density of states for a Ni solid. (Clearly, also the average density of states for a NiO is higher than the one for pure Ni, caused by the electronegativity of O.)

The local *d*-like DOS is hence the crucial parameter that will determine the overall probability for capture of an electron from the bulk into a specific state of the sputtered particle. From velocity measurements presented in a following

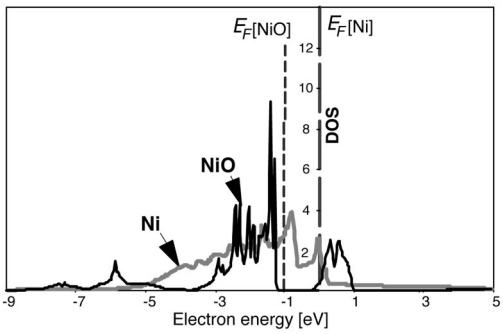

FIG. 4. Local density of states for *d*-like electrons for Ni[100] and NiO, respectively. The comparison is made between the DOS in the same sphere around the Ni core in both cases. The DOS around the Ni atom is more energy dependent for NiO; in particular, in the energy window we are interested in (2–3 eV below the Ni Fermi energy) the local DOS is higher. This is clearly valid also for the average DOS within the bulk (not shown), as electrons stay preferably close to oxygen atoms.

section we must conclude that the net effect is an increased capture cross section. In order to explain the reduction of the total yield in spite of the increased capture cross section, we must consider that the sputtering yield of Ni atoms from oxidized surfaces will be lower than for clean surfaces. This will reduce the total yield of sputtered Ni atoms.

It should be mentioned that a strong population reduction for some high-lying states has been previously observed[30] and can be interpreted within the resonant electron transfer picture. The presence of an oxide layer is known to increase the work function by approximately 1 eV. This is sufficient to shift the Fermi energy level energetically below high-lying excited states, around 1.5 eV above the atomic ground state, thus reducing the probability for tunneling into these states.

VI. STATE-SELECTIVE VELOCITY DISTRIBUTIONS OF METASTABLE Ni ATOMS

A. Interpretation of velocity spectra

Velocity distributions of sputtered atoms contain detailed information about the mechanisms involved in the emission process. This kind of information is especially helpful to identify viable inelastic processes.

We will disregard the possibility that the excitation takes place during the development of the collision cascade in the bulk; this is a generally accepted assumption, supported by the consideration that excited atoms have very short lifetimes in the bulk (10^{-12} s), mainly due to their large size. This is definitely true for highly excited states; for low-lying states, this might not be necessarily true.

A plausible scenario (i) can be described as follows. The emission of an ionic core is followed by electron capture into one of the electronic states of the ion at a distance from the surface that is determined by the overlap of the bulk and atomic wave functions. The overlap itself will depend on the velocity of the escaping particle and hence determine the capture cross section.

Clearly, the electron transferred to the atom still has a nonzero probability to tunnel back to the solid and eventually back again to the atom, until the free atom reaches a distance large enough to avoid further interaction between the emitted particle and the solid. However, since this situation involves the transfer of multiple electrons, the total probability will be very low.

In another scenario (ii) one might start with an inelastic energy transfer in the last collision of the cascade followed by a nonradiative deexcitation process during the escape. Again the velocity of the atom and the overlap of the wave functions will be crucial for the (*in this case*) electron tunneling cross section from the atom into the solid.

An emphasis of atoms with low velocities can be expected for the first scenario, while atoms with high velocities will more probably survive in the other case. Hence the measurement of the velocity spectra will enable us to distinguish between the two cases.

At this point a comment on experimental velocity spectra is useful. In many cases it is already helpful and informative to measure changes of the velocity spectrum as a function of a particular parameter variation, such as the surface oxidation. Thus we can easily obtain information about, e.g., an enhancement of the electron capture cross section for the particular parameter change. It is, however, very important to be able to relate the spectra under various conditions to a well known reference velocity distribution in order to be able to distinguish between scenarios (i) and (ii) mentioned above. To make this more clear, let us assume that we know the velocity spectrum for a situation where inelastic processes are absent and the entire sputter process is due to elastic collisions. Then the well known Sigmund-Thompson formula (1) applies where $f_{coll}(v)$ describes the particle density. The parameter v_b is the velocity corresponding to the surface binding energy

$$f_{coll}(v) \propto \frac{v^3}{(v^2+v_b^2)^3}. \tag{1}$$

Equation (1) has to be modified for cases where inelastic processes come into play. Scenario (i) described above would result in an adjusted distribution $f_{inel,1}(v)$,

$$f_{inel,1}(v) \propto \frac{v^3}{(v^2+v_b^2)^3}(1-e^{-a/v}) = f_{coll}(1-e^{-a/v}). \tag{2}$$

For scenario (ii) we would expect a distribution $f_{inel,2}(v)$, which is shifted in the opposite direction (*high energies*) on the v axis,

$$f_{inel,2}(v) \propto \frac{v^3}{(v^2+v_b^2)^3} e^{-a/v} = f_{coll} e^{-a/v}. \tag{3}$$

The parameter a in Eqs. (1)–(3) represents the electron tunneling probability, which can be assumed to be proportional to the density of states in the solid $n_{e,solid}$ at the particular energy of the atomic (ionic) level and the electron tunneling cross section $\int \psi^*_{solid} H_{exch} \psi_{ion,atom}$. It can be written in the form

$$a \propto n_{e,solid} \int \psi^*_{solid} H_{exch} \psi_{ion,atom}. \tag{4}$$

For the results, which we will present in the following, we will evaluate the spectra in relation to the reference spectrum (1) and with the assumption that the parameter v_b is well described by the surface binding energy of Ni of 4.2 eV.

For the analysis of the measured velocity distributions they have been compared with simulated spectra produced by a Monte Carlo computer program reproducing the experiment by assuming taht (a) the ejected particles are purely collisional and can be described by a velocity distribution (1), (b) atoms are emitted randomly and independently from each other, and (c) the specific geometry and other parameters of the experiment. From the best fit of the computer generated to the experimental data the free parameter v_B has been obtained. v_B is directly related to U_B, the surface binding energy of the emitted atoms if the process is purely collisional. A deviation of U_B from the expected surface binding energy, *generally set equal to the heat of sublimation*, is an indication that electronic processes are involved.

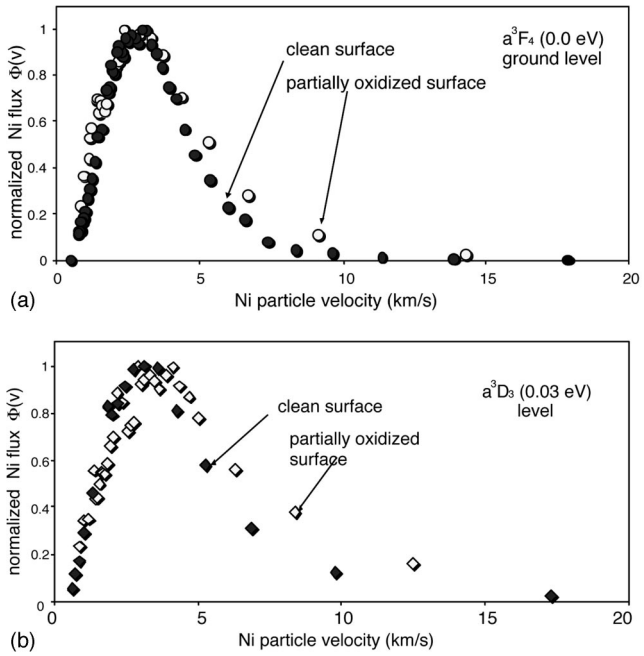

FIG. 5. Velocity distributions of sputtered Ni atoms in the (a) ground state and (b) $a\ ^3D_3$ metastable state for a clean as well as a partially oxidized Ni surface. The signals are normalized to one in the maxima of the distributions. If only elastic collisions were contributing, a fit according to formula (1) should yield the surface binding energy of Ni of 4.2 eV. Values deviating from this number [for details see Eq. (2)] indicate the influence of inelastic processes.

B. Influence of oxygen

From the considerations made in the preceding subsection it follows that the measurement of experimental velocity distributions of emitted atoms is of great importance. To simplify the rather complex situation described, we will initially compare distributions for atoms emitted in different metastable states and then for the same state for different surface conditions.

First of all, velocity distributions for the ground state $a\ ^3F_4$ and the $a\ ^3D_3$ state, both measured for a clean Ni surface and at room temperature, will be discussed. Later, these spectra will be compared with those obtained for the same states after oxygen exposure of the target.

By making the assumption, as discussed in Sec. VI A, that velocity distributions are described by a convolution of the Sigmund-Thomson distribution and an exponential function describing the neutralization probability, a deviation of the velocity distributions from the Sigmund-Thomson distribution with a parameter $U_B = 4.2$ eV is hence attributed to the second term in Eq. (2) or (3).

Thus differences observed for various electronic configurations or for different experimental parameters reflect modifications of the contribution of electronic processes. As far as clean metals at room temperature are concerned, the observation that velocity distributions measured for the metastable D_J states (Fig. 5) are broader than those corresponding to the ground state can be explained with a higher electron tunneling probability in a D_J state rather than in an F_J level. Recalling Eq. (2), the shift observed for the low-lying excited $a\ ^3D_3$ state is described by a larger a parameter.

A comparison with the spectra simulated according to the Sigmund-Thomson distribution has also been made to quantify the deviation from the case in which each emitted ionic core is neutralized (neutralization probability equal to one). By fitting the experimental data and leaving the parameter U_B as the only free one, the values 2.6 and 4 eV for the ground state and the low-lying metastable state have been deduced. These values are lower than the Ni sublimation energy of 4.2 eV that we would expect for a neutralization probability equal to one in both cases.

When comparing distributions obtained for the same metastable state with clean and oxidized surfaces, respectively, we can clearly observe that the velocity distributions for both levels shift to higher values for particles emitted from an oxidized surface. Disregarding effects due to different binding energies under surface oxidation, one of the most plausible hypotheses is that the shift observed is due to a higher tunneling probability for valence electrons from NiO than from metallic Ni.

By fitting the distributions obtained with oxidized surface, the best fitting value for the parameter U_B are 3 and 4.2 eV for the ground state and $a\ ^3D_3$, respectively. These values are much closer or even equal, within the experimental error, to the Ni sublimation energy than those corresponding to the clean Ni surface; the neutralization process during emission from an oxidized surface seems thus to be favored. This behavior can be explained qualitatively when we recall the meaning of the parameter a in the exponential law for the tunneling probability.

At this point we should look once more at the electronic properties of a Ni solid and compare them with those for a NiO sample, as previously made concerning the effect of the oxygen coverage on the velocity distrubutions. We will in this context consider the region at approximately 2.7 eV below the Fermi energy of Ni and take into account, for the reasons outlined in Sec. VI B, the local d-like DOS for Ni and NiO, respectively.

As noticed before, the local d-like DOS is higher for a NiO sample than the corresponding density of states for a Ni solid. The velocity spectra presented above can therefore be explained by an increased electron tunneling probability as a consequence of the surface oxidation.

C. Influence of target temperature

Let us recall that the yield of neutral emitted atoms, shown in Fig. 1, stays practically constant up to approximately 600 °C, while it decreases abruptly above that value. It is interesting to look at the corresponding velocity distributions in these regions.

For this reason, we measured velocity distributions of Ni atoms sputtered in the ground and metastable states from a target at room temperature, 400 °C and 725 °C. The spectra at room temperature and 400 °C are, within the experimental error, identical. The distributions corresponding to 400 °C and 725 °C are shown in Figs. 6 and 7.

It is clearly visible that the state-specific kinetic energy spectra for neutral Ni atoms shift to lower velocities for temperatures above 600 °C, which corresponds to the region where we observed the strong signal decrease.

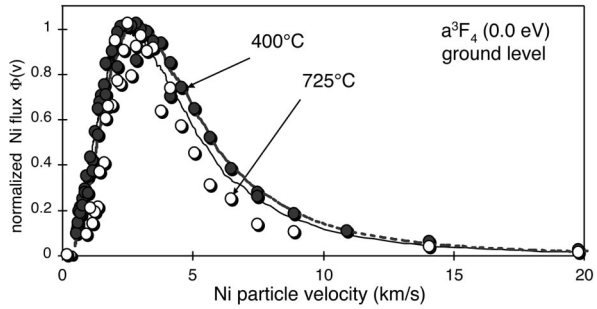

FIG. 6. Velocity distributions of sputtered Ni atoms in the ground state for a clean Ni surface at different temperatures. The signals are normalized to one in the maxima of the distributions. If only elastic collisions were contributing, a fit (full lines in the figure) according to formula (1) should yield the surface binding energy of Ni of 4.2 eV. Values deviating from this number indicate the increasing influence of inelastic processes at high temperatures. Furthermore, the fit becomes worse for increasing deviations from Eq. (1).

The parameter v_B at temperatures above 600 °C obtained from the comparison with the simulation program is slightly lower than for atoms emitted up to 600 °C, where we believe that the surface is partially covered with carbon. In other words, Ni atoms are either less tightly bound to the crystal at carbonized surface (*this seems to be in contradiction with the fact that the sputter yield of metal carbides is generally lower than for the metal*) or the electronic configuration due to carbon on the surface is changed in such a way that the electron tunneling into the $a\ ^3F_4$ and $a\ ^3D_3$ states becomes less probable. According to Eq. (4), this again can be caused by either a decreased $n_{e,solid}$ (DOS) or a decreased $\int \psi^*_{solid} H_{exch} \psi_{ion,atom}$ wave function overlap for the low-lying levels. The question is now if the tunneling probability decreases for all levels, thus producing a higher emission of secondary ions, or if higher-lying levels are favorably emitted by increasing target temperature.

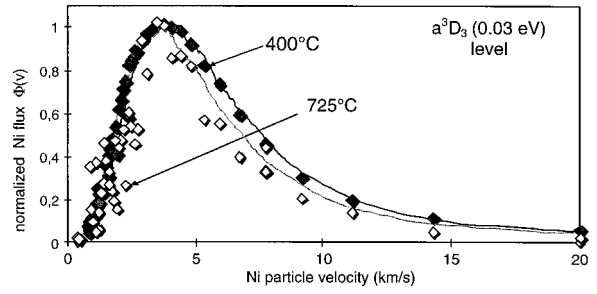

FIG. 7. Velocity distributions of sputtered Ni atoms in the $a\ ^3D_3$ metastable state for a clean Ni surface at different temperatures. The signals are normalized to one in the maxima of the distributions. If only elastic collisions were contributing, a fit (full lines in the figure) according to formula (1) should yield the surface binding energy of Ni of 4.2 eV. Values deviating from this number indicate the increasing influence of inelastic processes at high temperatures. Furthermore, the fit becomes worse for increasing deviations from Eq. (1).

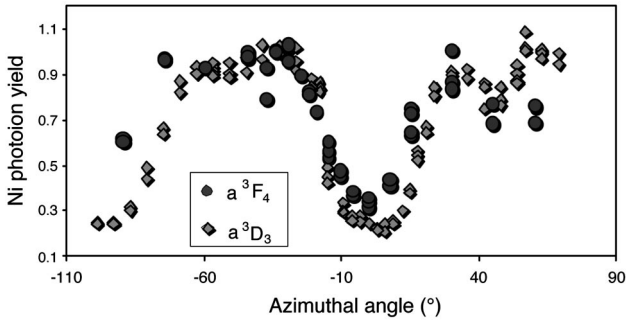

FIG. 8. Azimuthal angular dependence of neutral Ni atoms emitted in the ground state and $a\ ^3D_3$ metastable state, respectively. The curves are normalized to the maximum of the ground state distribution. The [110] direction corresponds to an azimuthal angle of 0° (primary minimum) and the [111] direction to an azimuthal angle of $\pm 45°$ (secondary smaller minimum).

VII. ANGLE OF INCIDENCE DEPENDENCE OF STATE-SPECIFIC EMISSION YIELD

A. Sputter yield

In order to study in more detail possible influences of the crystallography, we have studied for a Ni[100] single crystal the azimuthal angle of incidence dependence of sputtered neutral Ni atoms emitted in the $a\ ^3F_4$ and $a\ ^3D_3$ metastable states. In a single crystal the density of atoms along a specific direction varies with the incidence direction. This variable atomic density will introduce nonrandom effects in the collision sequence; therefore, we expect that both the sputtering yield and emission velocity will be sensitive to changes of the projectile angle of incidence. Whether also the electronic processes are influenced by the crystallography represents an issue worth studying in greater detail.

As discussed previously, excitation processes taking place in the collisional cascade can be excluded. We are thus allowed to describe the cascade assuming that all collisions are elastic. If this is the case, the incidence angle should not affect the electronic configuration of atoms or ionic cores involved in the cascade and we expect that the population density of ionic cores set in motion does not show directionality effects.

This is still far from excluding that directionality effects can show up. Actually, direction- or position-dependent bulk or surface properties (i.e., the DOS) can come into play in the last steps of the process, either in the last collision or in the emission process, the one that leads to excitation. If we recall that the bulk and the surface density of states generally show different trends for different electronic states (*valence s-like, p-like, or d-like electrons generally here different amplitudes*), directionality effects in the population density of emitted atoms could be attributed to these properties.

We bombarded Ni[100] with 8 keV Ar^+ at 45° to the target normal and rotated the crystal around the [100] axis. Some experiments in the past two decades have focused on this subject, where the yield dependence on the incidence polar angle[37] was studied. Otherwise, most documented experiments were devoted to the detection of angular distributions of emitted atoms at a constant incidence angle.[38]

In Fig. 8 the state-selective yield dependence on the azimuthal incidence angle is shown. The levels observed are

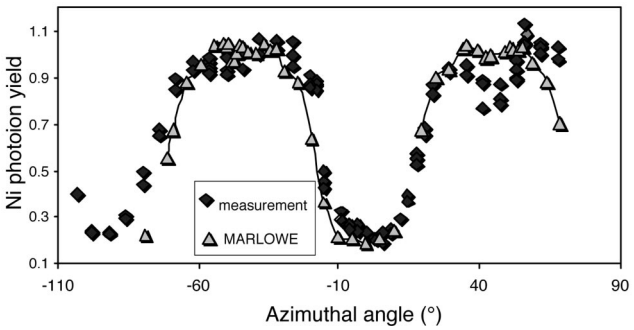

FIG. 9. Comparison of measured azimuthal angular dependence of neutral Ni atoms emitted in the $a\ ^3D_3$ metastable state with a MARLOWE computer simulation. The curves are normalized to the maximum of the experimental data. The [110] direction corresponds to an azimuthal angle of 0° (primary minimum) and the [111] direction to an azimuthal angle of ±45° (secondary smaller minimum).

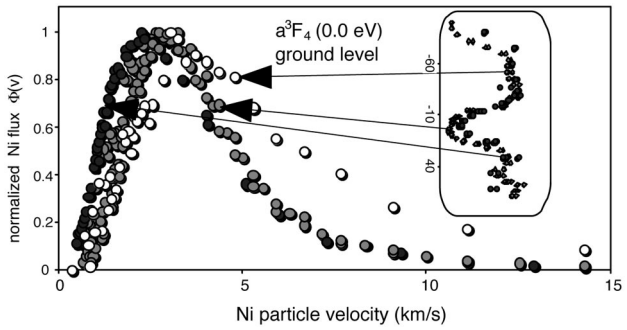

FIG. 10. Velocity distributions of sputtered Ni atoms in the ground state for a clean Ni surface for various azimuthal angles of the ion beam incidence. The signals are normalized to one in the maxima of the distributions. The inset shows the azimuthal angles for which the velocity spectra have been taken (see also Fig. 9).

again the ground state and one low-lying D_J level. The behavior of the curves is very similar for the two states and will be qualitatively discussed in the following sections. A slight difference in the maximum and minimum ratios can be observed and, if significative, can actually be explained only by assuming that the sputtering probability into a particular level is related to the electronic configuration and to direction-dependent properties of the matter.

The MARLOWE[39] program [*based on the binary collision approximation* (BCA)] was used to simulate collision events in a crystalline medium for different incidence azimuthal angles. Results are shown in Fig. 9 together with the experimental data corresponding to the initial state $a\ ^3D_3$. As seen in Fig. 9, the agreement between the experimental data and the computer simulation is rather good.

B. Emission kinetic energy from Ni[100] and from Ni polycrystal

We have hence observed that directionality effects in the sputtering yield show up and the characteristic trend observed is also reproduced by MARLOWE.[39] Concerning this method, we should notice that the binary collision approximation is a method that describes the trajectories of moving particles within a crystalline structure, by implementing atom-atom collisions. The good agreement between experimental points and simulated curves is hence, by itself, proof of the predominant role of elastic processes during the cascade. However, we see only the final result of cascade and emission; for instance, the slight difference between the trend shown by the ground state and the excited $a\ ^3D_3$ state can only be explained, in this context, by making the hypothesis that mechanisms other than the elastic collisions described by the BCA come into play, presumably during the emission process. This inelastic energy mechanism could hence favor the tunneling in a specific configuration, related to the corresponding density of states.

The strong dependence of the yield from the incidence direction and the state-specific trends have additional meaning. It has often been argued that, after the projectile incidence, the sputtering site should be described as an amorphous rather than as a crystalline ordered structure. During the cascade, in fact, the crystalline structure is locally destroyed in the cascade volume and it is consequently impossible to apply the concept of the density of states to this system. In particular, the local density of states can undergo strong variations, due to the aperiodicity introduced. Despite the validity of these considerations, the data reported above distinctively show that a strong remembrance of the crystalline structure is still observable in the sputtering process.

If we consider the typical developing time of the collisional cascade (picoseconds) and the time difference between the projectile incidence and the emission of the first sputtered particles (0.1 ps), it follows that the sputtered particles are emitted before the ordered structure becomes amorphous. In this cases, the emitted particles interact with a structure that has not yet been strongly altered by the cascade.

The aim of the present work is to find qualitatively an explanation for the origin of excited sputtered atoms. Thus, applying to the sputtering site physical properties, such as the density of states, which are rigorously valid only for a crystalline structure must be done with care.

Within the aim to identify effects that can be related to the original electronic configuration of the crystal, we measured also the emission velocities for atoms detected in different low-lying metastable states. The velocity distributions corresponding to the ground and low-lying metastable states are shown in Figs. 10 and 11. It can be seen that when the ion incidence is close to a crystallographic open direction, for instance, along [110] (corresponding to an azimuthal, angle of 0° in Figs. 8–11) and [111] (corresponding to an azimuthal angle of ±45° in Figs. 8–11), particles show in general higher emission energies than when the incidence is aligned with close-packed crystallographic orientations (corresponding to an azimuthal angle of ±30° in Figs. 8–11).

According to the model outlined in the present paper, we expect to observe in the velocity distributions deviations from the Sigmund-Thompson distribution in the case in which inelastic processes take place. For this reason, the distributions were fitted with the simulation program based on the Sigmund-Thompson distribution and the best-fitting values for the binding energy compared with the expected value of 4.2 eV (heat of sublimation). Furthermore, these values were compared for the same state and for the case in which a

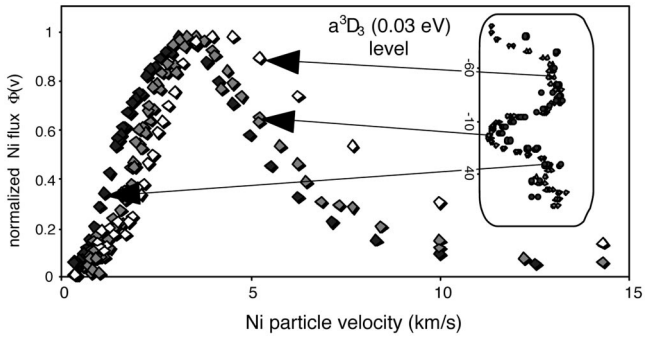

FIG. 11. Velocity distributions of sputtered Ni atoms in the $a\ ^3D_3$ metastable state for a clean Ni surface for various azimuthal angles of the ion beam incidence. The signals are normalized to one in the maxima of the distributions. The inset shows the azimuthal angles for which the velocity spectra have been taken (see also Fig. 9).

polycrystalline target and a single crystal at different incidence were used. This comparison is schematically summarized in Fig. 12.

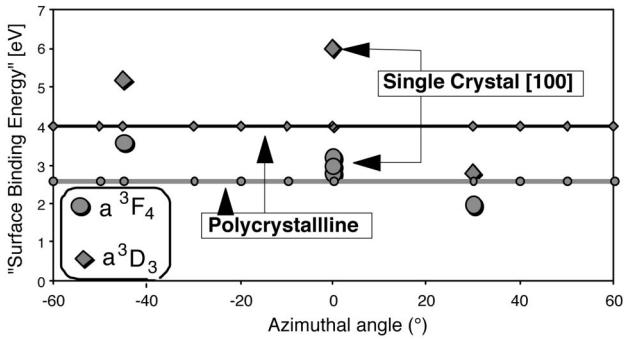

FIG. 12. Surface binding energies U_B obtained from fitting the experimental distributions under the assumption of the validity of Eq. (1) taking into account the experimental parameters.

VIII. CONCLUSIONS

In the present work, results concerning the emission of neutral atoms in different low-lying metastable states have been presented. In particular, we have focused attention on the population partition and emission velocities of atoms detected, $2-4$ mm away from the emission spot, in different electronic states. The influence of adsorbates, crystallographic direction, and target temperature on the emission velocity and on the energetic spectrum of emitted neutral were a crucial point in the discussion above.

The motivation of the present work is the desire to identify and describe qualitatively inelastic processes involved in the sputtering, such as an energy transfer mechanism that could explain the astonishingly high amount of atoms emitted in excited states. The measurements realized were aimed at identifying the cases in which inelastic mechanisms have been involved. A model, originally suggested by Veje, where an electron tunneling process can take place between an emitted ionic core and the solid has been used as the basis to explain the data.

For this purpose the energy spectrum of emitted atoms was compared with results obtained with a simulation model that assumes exclusively collisional processes. Inelastic processes were identified by deviations of the data from these fits. This picture relies strongly on the hypothesis that a relation between surface and solid properties, such as the density of states, and the efficiency of inelastic transfer energy exists.

ACKNOWLEDGMENTS

We acknowledge the financial support of the Austrian Science Foundation, FWF, Project NO. P10928-PHY. We would also like to thank P. Blaha for providing DOS calculations for Ni and NiO.

[1] H. Oechsner, Phys. Rev. Lett. **24**, 583 (1970).
[2] P. Sigmund, Phys. Rev. **184**, 383 (1969)
[3] M.W. Thompson, Philos. Mag. **18**, 377 (1968)
[4] G. Betz, R. Kirchner, W. Husinsky, F. Rüdenauer, and H.M. Urbassek, Radiat. Eff. Defects Solids **130/131**, 251 (1994).
[5] G. Nicolussi, W. Husinsky, D. Gruber, and G. Betz, Phys. Rev. B **51**, 8779 (1995).
[6] W. Berthold and A. Wucher, Nucl. Instrum. Methods Phys. Res. B **115**, 411 (1996).
[7] A. Wucher and Z. Sroubek, Phys. Rev. B **55**, 780 (1997).
[8] W. Husinsky, A. Cortona, V. Schmidt, and G. Betz, Izv. Akad. Nauk Ser. Fiz. **62**, 710 (1998).
[9] C. He, S. Rosencrance, Z. Postawa, C. Xu, R. Chatterjee, D.E. Riederer, B. Garrison, and N. Winograd, Nucl. Instrum. Methods Phys. Res. B **100**, 209 (1995)
[10] C. He, Z. Postawa, S. Rosencrance, R. Chatterjee, B. Garrison, and N. Winograd, Phys. Rev. Lett. **75**, 3950 (1995).
[11] E. Vandeweert, V. Philipsen, W. Bouwen, P. Thoen, H. Weidele, R. Silverans, and P. Lievens, Phys. Rev. Lett. **78**, 138 (1997).
[12] W. Husinsky and G. Betz, Scanning Microsc. **1**, 1603 (1987).
[13] G. Betz and W. Husinsky, Nucl. Instrum. Methods Phys. Res. B **32**, 331 (1988).
[14] G. Betz, Nucl. Instrum. Methods Phys. Res. B **27**, 104 (1987).
[15] E. Veje, Phys. Rev. B **28**, 5029 (1983).
[16] W. Husinsky, G. Betz, B. Strehl, P. Wurz, K. Mader, and K.H. Krebs, Nucl. Instrum. Methods Phys. Res. B **19/20**, 92 (1987).
[17] I. Tsong and N. Yusuf, Nucl. Instrum. Methods **170**, 357 (1980).
[18] I. S. T. Tsong, *Inelastic Ion Solid Collisions*, edited by E. Taglauer and W. Heiland, Springer Series in Chemistry and Physics Vol. 17 (Springer, Berlin, 1981), p. 238.
[19] S. Dzioba and R. Kelly, Surf. Sci. **100**, 119 (1980).
[20] S. Dzioba, O. Auciello, and R. Kelly, Radiat. Eff. **45**, 235 (1980).
[21] W. Husinsky, R. Bruckmüller, P. Bum, F. Viehböck, D. Hammer, and E. Benes, J. Appl. Phys. **48**, 4734 (1977).
[22] W. Husinsky, G. Betz, and I. Girgis, Phys. Rev. Lett. **50**, 1689 (1983).
[23] W. Husinsky, J. Vac. Sci. Technol. B **3**, 1546 (1985).
[24] M.L. Yu, D. Grischkowsky, and A.C. Balant, Phys. Rev. Lett. **48**, 427 (1982).

[25] M.W. Thompson and R.S. Nelson, Philos. Mag. **7**, 2015 (1962).
[26] G. S. Hurst and M. G. Payne, *Principles and Applications of Resonance Ionization Spectroscopy* (Hilger, Bristol, 1988).
[27] M.J. Pellin, Pure Appl. Chem. **64**, 591 (1992).
[28] P. Lievens, E. Vandeweert, P. Thoen, and R. Silverans, Phys. Rev. A **54**, 2253 (1996).
[29] W. Husinsky, G. Nicolussi, and G. Betz, Nucl. Instrum. Methods Phys. Res. B **82**, 323 (1993).
[30] E. Vandeweert, Ph.D. thesis, University Leuven, 1997.
[31] R. Kelly, Phys. Rev. B **25**, 700 (1982).
[32] M.L. Yu, Nucl. Instrum. Methods Phys. Res. B **18**, 542 (1987).
[33] B.I. Craig, J.P. Baxter, J. Singh, G.A. Schick, P.H. Kobrin, B.J. Garrison, and N. Winograd, Phys. Rev. Lett. **57**, 11 (1986).
[34] P. Homolka, W. Husinsky, G. Nicolussi, G. Betz, and X. Li, Phys. Rev. B **51**, 4665 (1995).
[35] G. Nicolussi, W. Husinsky, and G. Betz, Phys. Rev. Lett. **71**, 1518 (1993).
[36] P. Blaha, K. Schwarz, and J. Luitz, WIEN97, Vienna University of Technology, 1997 [updated Unix version of P. Blaha, K. Schwarz, P. Sorantin, and S.B. Trickey, Comput. Phys. Commun. **59**, 399 (1990)].
[37] G. Betz and K. Wien, Int. J. Mass Spectrom. Ion Processes **140**, 1 (1994).
[38] Chun He, Z. Postawa, A.M. El-Maazawi, S. Rosencrance, B.J. Garrison, and N. Winograd, J. Chem. Phys. **100**, 6226 (1994).
[39] W. Eckstein, *Computer Simulation of Ion-Solid Interactions* (Springer-Verlag, Berlin, 1991).